JOURNAL OF MATERIALS SCIENCE 19 (1984) 1000–1006

Magnetic measurements on iron-rich amorphous alloys containing chromium: Mössbauer study and *B–H* loops

M. HENRY, M. BOURROUS, F. VARRET
ERA 682, Faculté des Sciences, 72017 Le Mans Cedex, France

P. FOURNIER
Pont a Mousson Sa, 91 av. de la Libération, 54017 Nancy Cedex, France

We present results concerning the magnetic properties of some iron-rich amorphous alloys containing from 0 to 8 at% chromium obtained as 2 mm wide, quenched ribbons. Basically, the Curie temperature and magnetization are sizeably decreased by chromium additions, but the low-field permeability is increased.

1. Introduction

Due to their high magnetic permeability and their good mechanical properties transition metal–metalloid amorphous alloys are suited to magnetic applications such as magnetic shielding [1–4]. But the use of amorphous iron-based alloys can be limited by their corrosion behaviour. It has been shown that chromium addition in these alloys highly increases their corrosion resistance [5–7].

The present paper shows that chromium in amorphous $(Fe_{80-x}Cr_x)(PC)_{20}$ alloys also has sizeable effects on their magnetic properties. Chromium concentration has been varied in the range 0 to 7.6 at%.

2. Samples

The amorphous samples were produced in the Saint Gobain Recherche Laboratories by using the well known melt spinning technique. The ribbons were about 2 mm wide and $(30 \pm 5)\,\mu$m thick. The different parameters of importance for geometry were previously studied [8]. The experimental conditions were identical and constant for all samples: compositions are presented in Table I in atomic per cent.

Two kinds of alloys were studied, having either carbon (samples 1 and 5) or phosphorus (the others) as the prominent metalloid.

The amorphous state of the samples was verified by X-ray diffractometry and differential thermal analysis. The crystallization temperatures are reported in Table I.

X-ray diffraction shows that dull faces (wheel side surface) were completely amorphous; for samples 1 and 5, two peaks were observed on the shiny face (air side surface) corresponding to a small amount of crystalline phase. This fact agrees with a previous study [9] of the critical ribbon thickness in amorphous Fe–P–C alloys. Ribbons were kept at room temperature. All measurements were made on as-quenched ribbons.

3. Mössbauer spectroscopy analysis

The Curie temperature, hyperfine field and spin-texture were studied as functions of chromium concentration. Mössbauer samples of π cm^2 were obtained by setting ribbon pieces side by side without sticking, to avoid strains on the material.

3.1. Curie temperature (T_c)

Mössbauer spectra of amorphous alloy without chromium (4), run at room temperature and at 370° C, as shown in Fig. 1, are typical of iron-rich amorphous alloys, according to the literature.

By thermal scanning of the paramagnetic line, the Curie temperature (Table I) of all the amorphous alloys were determined. It decreases when the chromium content is increased (Fig. 2), in agreement with the literature [11]. However the substitution of carbon atoms by larger phosphorus

0022–2461/84 $03.00 + .12

TABLE I Alloy compositions (in at%), crystallization temperatures, (obtained at DTA at 500° C h^{-1}), and Curie temperatures

Sample	Cr	P	C	$T_{crystallization}$ (° C)	T_{Curie} (° C)
1	7.6	8.3	10.9	475	160 ± 6
2	6.5	13.2	7.8	485	155 ± 6
3	4.3	10.1	8.6	473	229 ± 3
4	0	12.2	8.5	452	330 ± 10
5	< 0.2	6.9	10.9	431	333 ± 10

metalloid atoms tends to increase the Curie temperature [10]. This substitution might be responsible for the "anomaly" concerning the 7.6/6.5 Cr at% alloys in Fig. 2.

Although the Mössbauer thermal scanning method is relatively slow with respect to more usual calorimetric methods, it has an advantage in its spectroscopy ability to provide information on sample homogeneity; in the present case, Fig. 2 shows that the transition temperature is unique and well defined. This gives evidence that none of the alloys studied exhibited microphase separation or similar inhomogeneity.

3.2. Hyperfine field distribution

Room temperature spectra are shown on Fig. 3. The broad lines, indicating a magnetic hyperfine field distribution, are computer fitted [12] by using a discrete distribution $P(H)$. The correct value for line intensities was established from the recordings of texture free spectra [13, 14]. The line width was close to the instrumental value (0.21 mm sec^{-1}), quadrupole shift was set to zero; isomer shift was fitted to an unique value; the weights of the sextets were fitted to give the rough $P_i(H)$ distribution. Smoothing by the law $P_i' = (P_{i+1} + 2P_i + P_{i-1})/4$ was systematically applied.

Once the whole procedure [15] was carefully applied, the experimental distribution $P(H)$ did not exhibit any particular structure (Fig. 4). It is clear that the lower part of $P(H)$ is disturbed by the quadrupole interactions, and actually might be much different.

As the chromium concentration is increased, $P(H)$ progressively shifts to lower H values, the average $\bar{H}$ values are listed in Table II.

3.3. Magnetic texture from Mössbauer spectroscopy

We previously proposed an accurate method of measuring line intensities in the case of overlapping lines using a linear combination of standard spectra [15]. Then the measured line intensities were used to determine three "principal populations" of the spins N_x, N_y, N_z which contains all information available from unpolarized Mössbauer experiments [17]. Such a method is applied here. Useful orientations of the γ beam with respect to the ribbon axis are shown in Fig. 5.

Fig. 6 shows the five spectra needed for spin texture determination:

– two standard spectra obtained as follows:

(i) ferromagnetic sample magnetically saturated along OX, observed perpendicularly to the (OX, OY) plane (H_{app} = 400 Oe)

(ii) a random spectrum obtained in (1 1 1) configuration (D, Fig. 5).

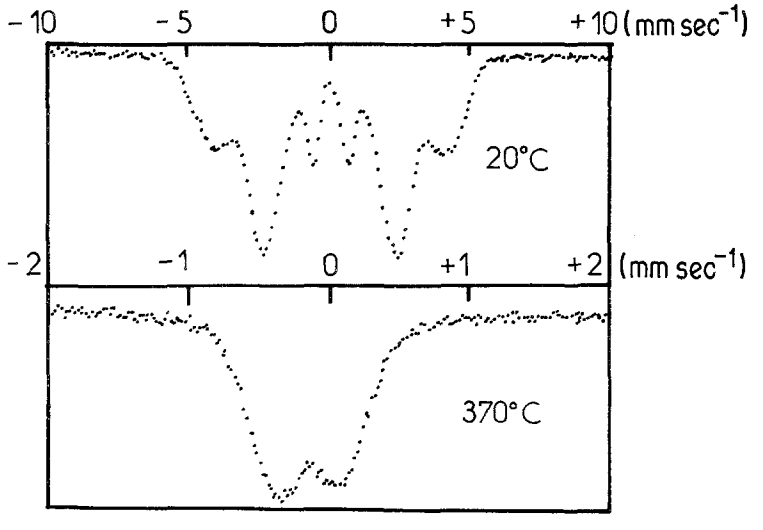

Figure 1 Mössbauer spectra of amorphous alloy 4 (cf. Table I).

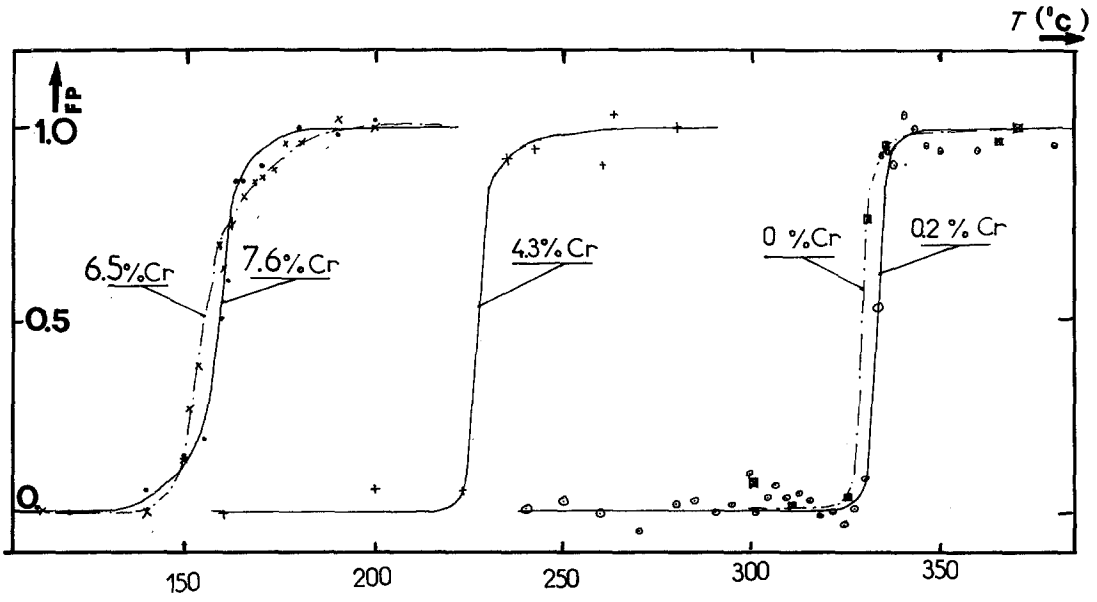

Figure 2 Curie temperature dependance for different chromium concentrations in iron-rich amorphous alloys (Velocity for Mössbauer scanning = ± 0.33 mm sec^{-1}). (FP: normalized depth of the paramagnetic lines).

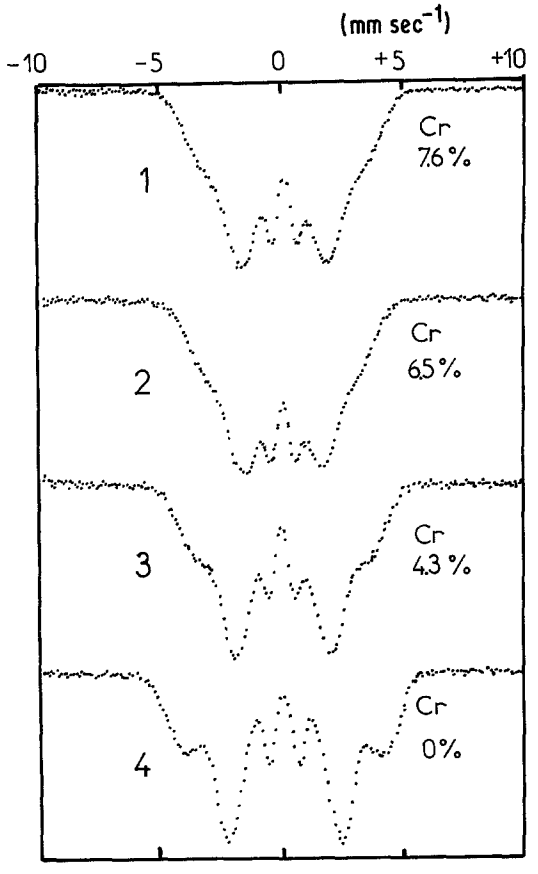

Figure 3 Experimental Mössbauer spectra at room temperature for different chromium concentrations in iron-rich amorphous alloys.

– three experimental spectra in configurations A, B, C without any applied field.

Table III presents results concerning texture. Row 6 gives the convenient check for testing the quality of the method [13, 14]. According to the observed departures from its expected value of 2/3, the accuracy of the method concerning $N_{x,y,z}$ is thought to be typically ± 0.03.

It can be observed from Table III that N_z always takes low values $\leqslant 0.2$. Therefore the in-plane anisotropy is relatively strong as compared with commercial 2826 MB Metglas studied in a similar way [18]. It is clear that the in-plane anisotropy might be related to both quenching conditions and magnetostrictive properties.

4. Hysteresis loops

4.1. Experimental device

Hysteresis loops were obtained by a standard technique. The amorphous sample consisted of one piece of ribbon 0.50 m long, having a negligible demagnetizing field. The magnetic field H was supplied by a 0.50 m long solenoid giving up to 2×10^4 A m^{-1}. The pick-up coil (2500 turns) was tightly wound around a thin rectangular tube closely surrounding the amorphous ribbon, to minimize the air contribution to the measured induction. The applied field variation was sinusoidal (50 Hz); the dB/dt signal from the pick-up

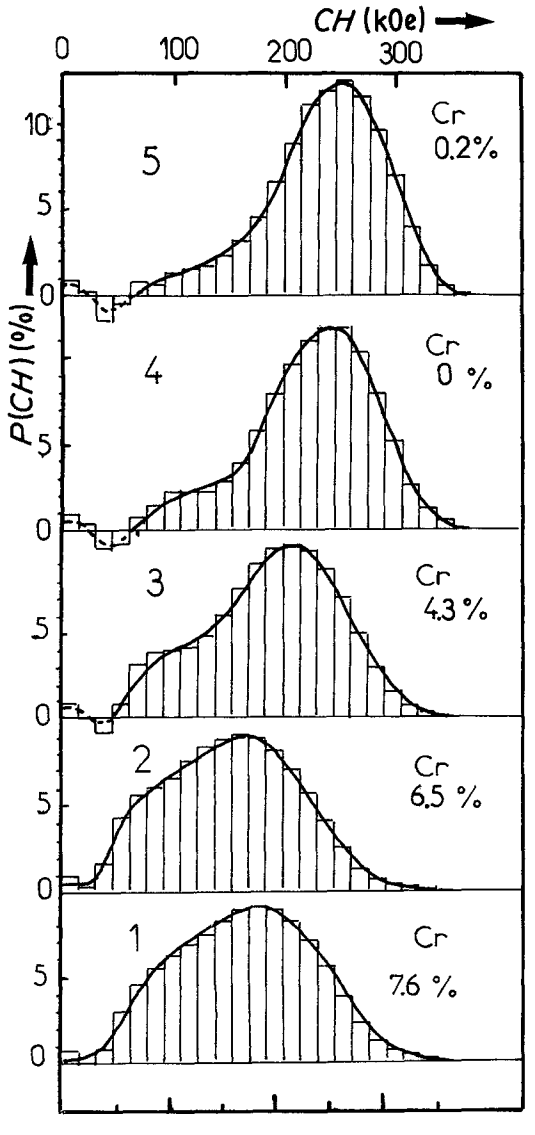

Figure 4 Hyperfine field distribution $P(H)$ of iron-rich amorphous alloys for different chromium concentrations.

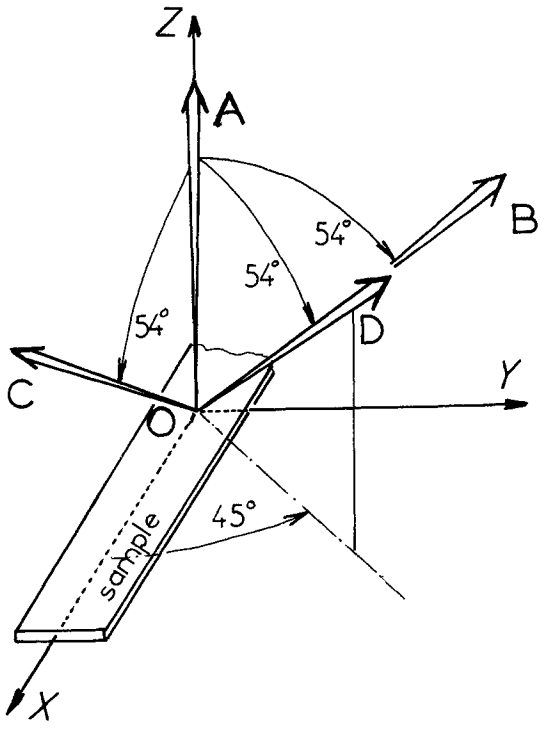

Figure 5 Set of principal axes in the case of a ribbon, and orientations of the radiation.

coil was sent to a $X-Y$ scope through a "home-made" amplifier-integrator circuit.

The air contribution was easily obtained by measuring the output signal without a sample.

4.2. Results

Fig. 7 shows hysteresis loops obtained for a given field amplitude, $H_{max} = 268\ A\ m^{-1}$.

Systematic measurements of the induction flux amplitude ϕ_{max} as a function of H_{max} were performed.

To express the resulting $\phi_{max} = S_r B_{max}$ in terms of induction amplitude B_{max}, the section area S_r had to be measured. The irregular shape of the section and the actual area S_r were carefully determined for one ribbon (Fig. 8); for all ribbons, however, we only determined the "apparent" section $S' = wt$ (width x thickness) and assumed that the ratio S_r/S' remained roughly the same for all pieces of all ribbons (~ 0.77). Then the results could be expressed in terms of "true"

TABLE II Mean hyperfine field for different chromium concentrations

Sample	Cr (at %)	$\langle H \rangle$ (kOe)
4	0	236
5	0.2	248
3	4.3	197
2	6.5	157
1	7.6	168

TABLE III Magnetic texture analysis

Sample	% Cr	N_x	N_y	N_z	$\langle\cos^2\theta_R\rangle_B + \langle\cos^2\theta_R\rangle_C$
1	7.6	0.44	0.38	0.18	0.642
2	6.5	0.45	0.35	0.20	0.640
3	4.3	0.53	0.42	0.05	0.625
4	0	0.61	0.34	0.05	0.647
5	< 0.2	0.62	0.38	0.00	0.687

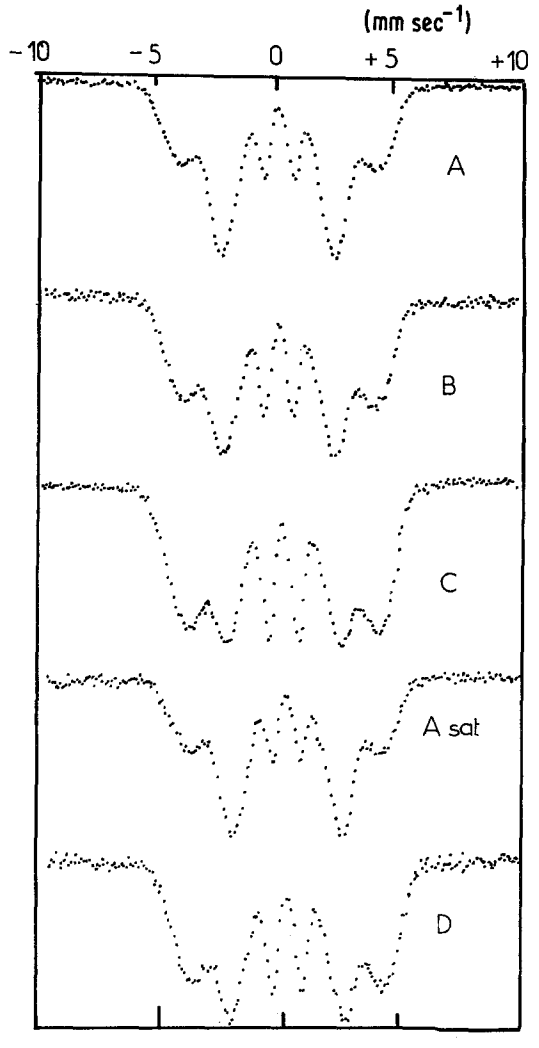

Figure 6 Mössbauer spectra taken at room temperature in different configurations [sample 4 (0 at % Cr)].

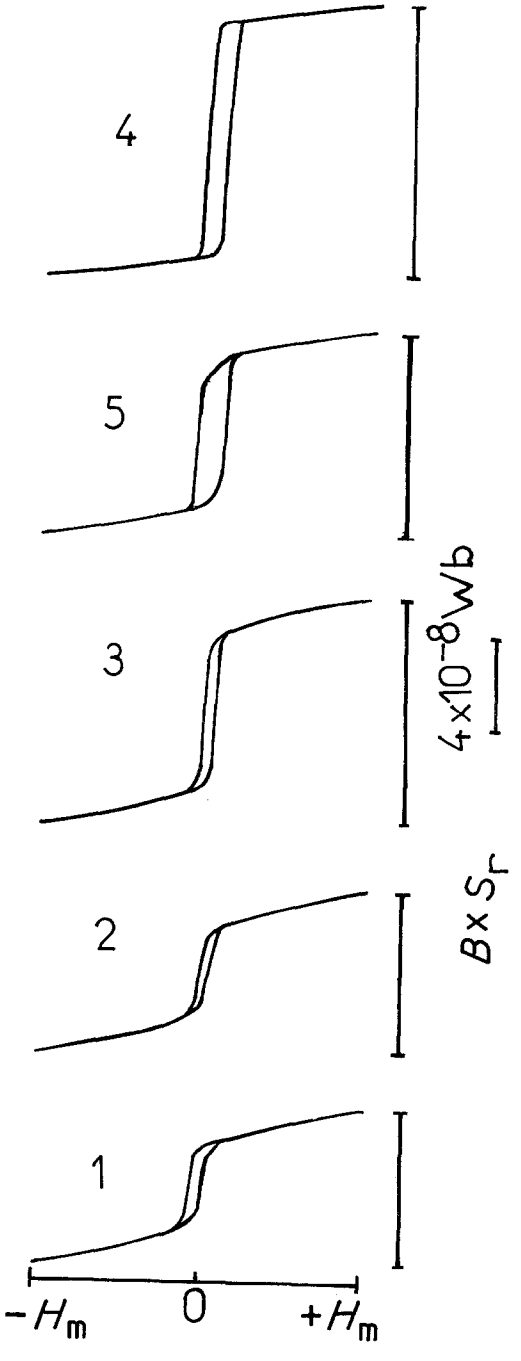

Figure 7 Hysteresis loops for $H_{max} = 268$ A m^{-1}.

induction (B) and of "apparent" induction (B') (only the latter is relevant for technical applications). For each hysteresis loop we note values B_{max} and H_{max} the maximum amplitudes of the magnetization and of the applied field, respectively. The curves $B_{max} = f(H_{max})$ are actually first magnetization curves: they are plotted in Figs. 9a and b.

5. Discussion

Analysis of Fig. 9 and Table II leads to the following conclusions:

(i) an increase in Cr-content (consider samples 4, 3, 2) lowers the Curie temperature, the average hyperfine field and saturation magnetization; on the other hand, the initial permeability is markedly increased.

(ii) substituting carbon by phosphorus (consider samples 5 → 4 and 1 → 2) has little effect on the Curie temperature, but sizeably lowers the average hyperfine field and saturation magnetization; the initial permeability is also increased.

The effect of chromium on low-field perfor-

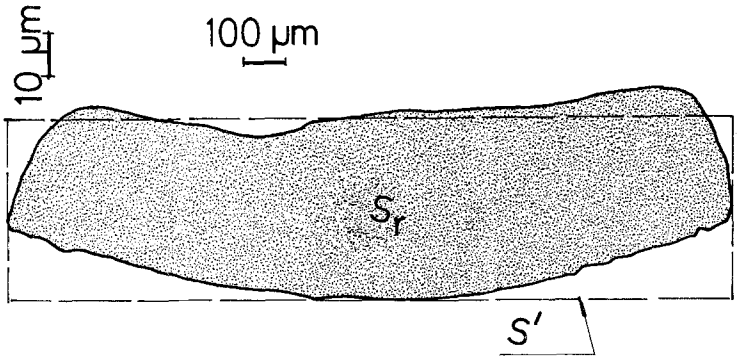

Figure 8 Profile of the ribbon section given by Talysurf investigations. Ribbon section S' = rectangular "apparent" area; S_r = actual ribbon section.

mances is illustrated by the progressive bending of hysteresis loops on Fig. 7.

No obvious conclusion can be presently drawn from the texture data which nevertheless exhibit noticeable differences.

6. Conclusion

Chromium additions are shown to influence magnetic properties of as-quenched iron, phosphorus, carbon amorphous ribbons.

Chromium-rich ribbons (> 4%) should be preferred for low-field applications (< 10 A m^{-1}), while chromium-poor ribbons should be better in larger fields, because of their larger saturation magnetization.

Acknowledgement

This work has received financial support from the French Ministry of Research and Industry.

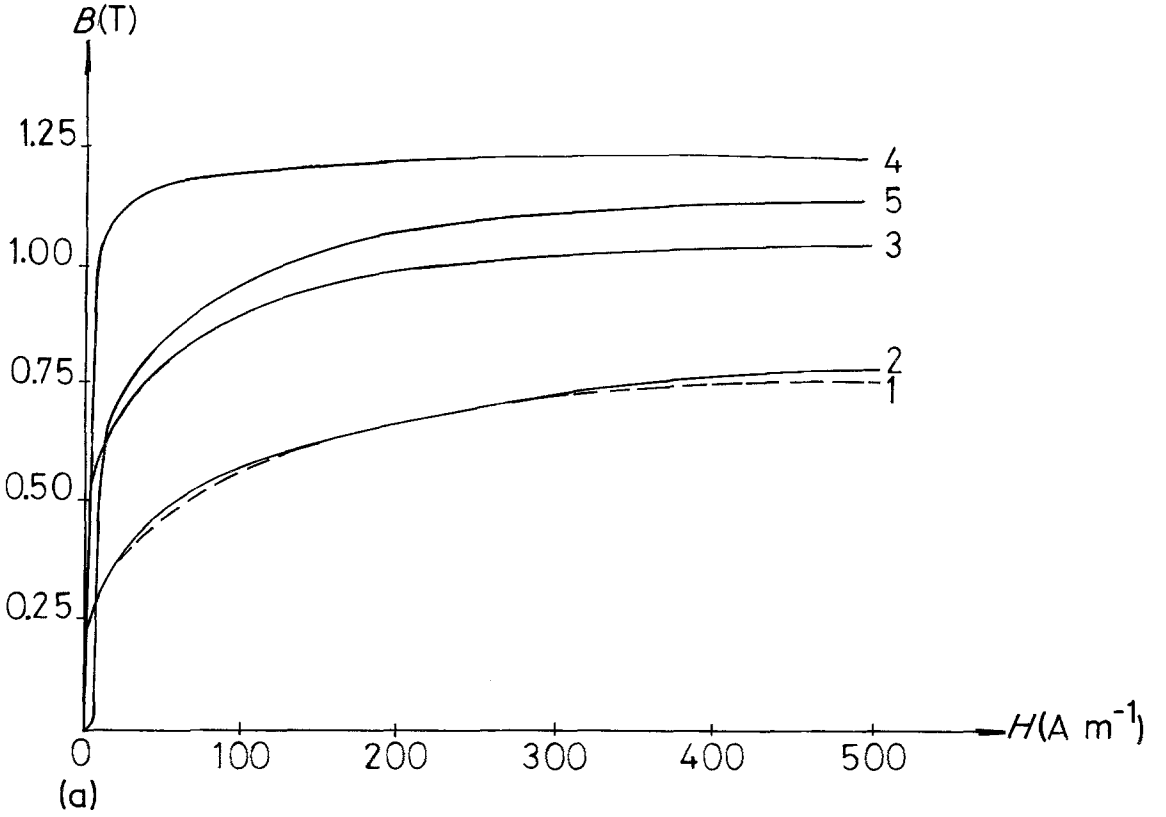

Figure 9 B_{max} as a function of H_{max}, from B–H loops: (a) large fileds; (b) weak fields.

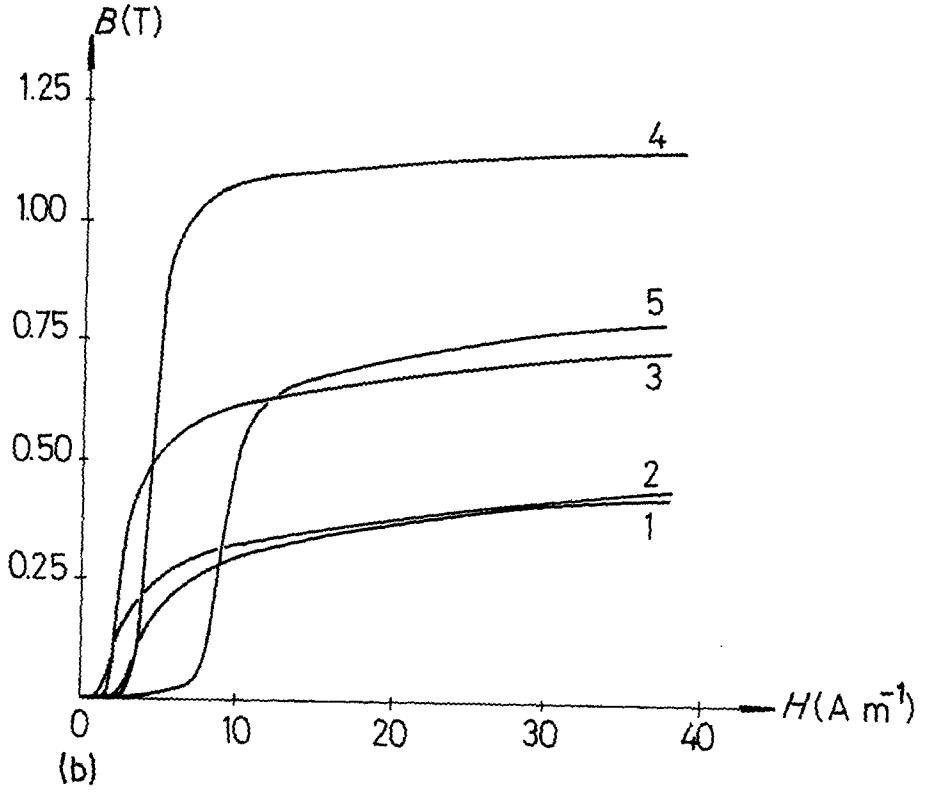

Figure 9 Continued.

References

1. C. D. GRAHAM and T. EGAMI, *J. Magn. Magn. Mater.* **15–18** (1980) 1325.
2. J. DURAND, *J. Phys.* **41** (1980) C8–609.
3. J. J. GILMAM, *ibid.* **41** (1980) C8-811.
4. H. VARLIMONT and R. BOLL, *J. Magn. Magn. Mater.* **26** (1982) 97–105.
5. C. M. HANHAM, Y. WASEDA and K. T. AUST, *Mater. Sci. Eng.* **45** (1980) 71.
6. M. NAKA, K. HASHIMOTO and T. MASUMOTO, *J. Jpn. Inst. Met.* **38**, (1974) 835.
7. M. NAKA, K. HASHIMOTO and T. MASUMOTO, *J. Non Cryst. Solids* **31** (1979) 355.
8. P. FOURNIER and M. HENRY, *RGE-FRA* **5** (1983) 314.
9. A. INOUE, M. HAGIWARA and T. MASUMOTO, *J. Mater. Sci.* **17** (1982) 180.
10. L. KABACOFF and S. DALLEK, *J. Non Cryst. Solids* **48** (1982) 375.
11. I. W. DONALD, T. KEMENY and H. A. DAVIES, *J. Phys. F.* **11** (1981) L131–6.
12. F. VARRET and J. TEILLET, Computer fitting programs (unpublished).
13. J. M. GRENECHE, M. HENRY and F. VARRET, International Conference on the Applications of the Mössbauer Effect (ICAME) Jaipur, 1981, published in Proceedings of the Indian National Science Academy (1982) pp. 900–902.
14. J. M. GRENECHE, Thèse, Paris VI (1981).
15. F. VARRET, ICAME, Jaipur, 1981, published in Proceedings of the Indian National Science Academy (1982) pp. 129–140.
16. J. M. GRENECHE, M. HENRY and F. VARRET, ICAME, Jaipur, 1981, published in Proceedings of the Indian National Science Academy (1982) pp. 908–911.
17. J. M. GRENECHE and F. VARRET, *J. Phys. C* **15** (1982) 5333.
18. J. M. GRENECHE, M. HENRY and F. VARRET, *J. Magn. Magn. Mater.* **26** (1982) 113.

Received 12 May
and accepted 21 July 1983